LETTERS

Allometric degree distributions facilitate food-web stability

Sonja B. Otto[1], Björn C. Rall[1] & Ulrich Brose[1,2]

In natural ecosystems, species are linked by feeding interactions that determine energy fluxes and create complex food webs. The stability of these food webs[1,2] enables many species to coexist and to form diverse ecosystems. Recent theory finds predator–prey body-mass ratios to be critically important for food-web stability[3–5]. However, the mechanisms responsible for this stability are unclear. Here we use a bioenergetic consumer–resource model[6] to explore how and why only particular predator–prey body-mass ratios promote stability in tri-trophic (three-species) food chains. We find that this 'persistence domain' of ratios is constrained by bottom-up energy availability when predators are much smaller than their prey and by enrichment-driven dynamics when predators are much larger. We also find that 97% of the tri-trophic food chains across five natural food webs[7] exhibit body-mass ratios within the predicted persistence domain. Further analyses of randomly rewired food webs show that body mass and allometric degree distributions in natural food webs mediate this consistency. The allometric degree distributions hold that the diversity of species' predators and prey decreases and increases, respectively, with increasing species' body masses. Our results demonstrate how simple relationships between species' body masses and feeding interactions may promote the stability of complex food webs.

Natural food webs are characterized by energy and biomass flows across various trophic levels. Despite the structural complexity of these large networks[8], simple food-chain motifs usefully represent

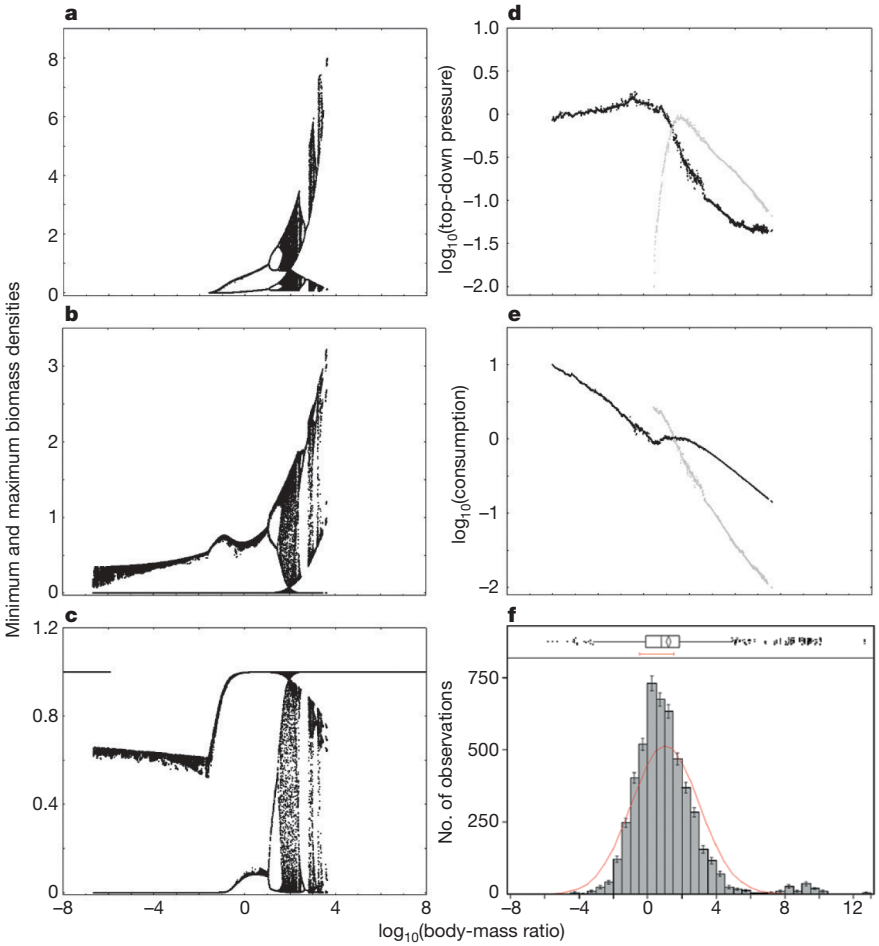

Figure 1 | Population dynamics in tri-trophic food chains. **a**–**c**, Effects of R on the biomass minima and maxima of top (**a**), intermediate (**b**) and basal (**c**) species. **d**, Effect of R on $\log_{10}$ of top-down pressure per unit biomass of prey, for intermediate–basal (black) and top–intermediate (grey) species. **e**, Effect of R on $\log_{10}$ of consumption per unit biomass of predator, for intermediate–basal (black) and top–intermediate (grey) species. **f**, Frequency distribution of empirical R in five natural food webs (means ± s.e.m.); the red line shows a normal distribution. An outlier box-plot is shown above the histogram. Simultaneous variation of R of top to intermediate and intermediate to basal species: when $R = 0$, all three species have equal size; when $R < 0$ and $R > 0$, predators are smaller and larger, respectively, than their prey.

[1]Darmstadt University of Technology, Department of Biology, Schnittspahnstrasse 10, 64287 Darmstadt, Germany. [2]Pacific Ecoinformatics and Computational Ecology Lab, Berkeley, California 94703, USA.

the energy transfer[9,10] and mechanisms responsible for non-equilibrium population dynamics in food webs[11–14]. Analyses of food-chain motifs illustrate how population stability under chaotic dynamics may be driven by high resource productivity[11], variation in the species' timescales[14] or certain body-mass ratios between consumers and resources[12]. Population persistence depends on parameters of energy gain (production and consumption) and loss (metabolism and mortality)[15], whose rates per unit biomass follow allometric negative-quarter power-law relationships with the average body masses of the populations[16,17]. We use a bioenergetic model based on these principles[6] to explore how the dynamics of top (t), intermediate (i) and basal (b) species of tri-trophic food chains changes with varying consumer–resource body-mass ratios (R). Our analyses predict the probability of stable coexistence of three invertebrate species in tri-trophic food chains depending on R, which is subsequently evaluated for food chains of five natural food webs[7].

We initially explored a tri-trophic system by simultaneously increasing R between top and intermediate species (R_{ti}) and between intermediate and basal species (R_{ib}) from 10^{-8} to 10^{8} (that is, the consumer is between 10^{8}-fold smaller and 10^{8}-fold larger than its prey). The simultaneous increase in both R values is a simplification to gain knowledge of the population dynamics. The minima and maxima attained for the biomass densities of the three species across this range of R (Fig. 1a–c) depict four distinct stages of coexistence. At the lowest R ($R \leq 10^{-6.7}$), the system exhibits a stable equilibrium where only the basal species persists. At higher R ($10^{-6.7} \leq R < 10^{-1.6}$), two stable attractors appear: either the basal species persists at equilibrium, or basal and intermediate species exhibit globally attractive limit cycles[14]. In this range of R, the top species is much smaller than its prey, and its mass-specific metabolic rate exceeds the energy available from consuming the intermediate species, which prevents persistence[15]. Increasing R above these low ratios decreases the metabolic rates per unit biomass of top and intermediate species and increases the intermediate species' biomass density until the top species' consumption exceeds its metabolic demand enough for the top species to persist ($R = 10^{-1.6}$). Further increases in R ($10^{-1.6} < R < 10^{3.5}$) increases top-down pressure on the intermediate species and decreases top-down pressure on the basal species (Fig. 1d). Increasing R within this range also increases the consumption rate per unit biomass of the intermediate species over that of the top species (Fig. 1e). This counterintuitive result is explained by the simultaneous decrease in the density of intermediate species and increase in the density of basal species, which enhances the energy availability per unit biomass to the intermediate species. This availability increases with R, leading to accelerating oscillations of top and intermediate species (Fig. 1a–c). Mechanistically similar to the 'paradox of enrichment'[18], the dynamics are driven from equilibrium through a series of bifurcations to more complex dynamics until the minimum density of the intermediate species drops below a critical extinction threshold, eliminating both consumer species ($R = 10^{3.5}$; Fig. 1). The complex dynamics in this range of R are caused by the different timescales of the three populations[14]. Further increases in R ($R > 10^{3.5}$) cause unstable dynamics that continue to prevent the persistence of the intermediate and top species (Fig. 1a–c). The persistence of all three species is thus bounded by energy availability to the top species at low R and by enrichment-driven instability of the intermediate species towards higher R.

With this mechanistic background on food-chain dynamics, we decoupled R of upper and lower trophic levels and independently varied both R_{ti} and R_{ib} between 10^{-6} and 10^{13}. This range corresponds to the range of empirical R values of the five natural food webs studied here (Fig. 1f). In 19.6% of this parameter space, we found persistence of all three species (Fig. 2, red areas). The energy-availability boundary of this persistence domain depends on R_{ib}, which needs to exceed a threshold ($R_{ib} > 10^{-1.6}$) within a broad range of R_{ti} ($R_{ti} > 10^{-4.3}$) to increase the density of the intermediate species (that is, the energy available) enough for the top species to persist (Fig. 2, left boundary of red areas). If R_{ib} and R_{ti} exceed a second threshold, both top and intermediate species cease to persist as a result of enrichment-driven dynamics (Fig. 2, right boundary of red areas). This enrichment boundary is determined more continuously and interactively by both R_{ib} and R_{ti} than the energy-availability boundary (Fig. 2).

The persistence domain in Fig. 2 implies that a tri-trophic food chain with R randomly chosen from the range $10^{-6} \leq R \leq 10^{13}$ has a 19.6% chance of persisting. However, 97.5% ± 4.1% (mean ± s.d.) of all invertebrate tri-trophic food chains across five natural food webs from different ecosystem types (see Methods) fall within the persistence domain (Fig. 2a, black points; Fig. 2d, black bars). This difference in probabilities clearly suggests that species' body-mass

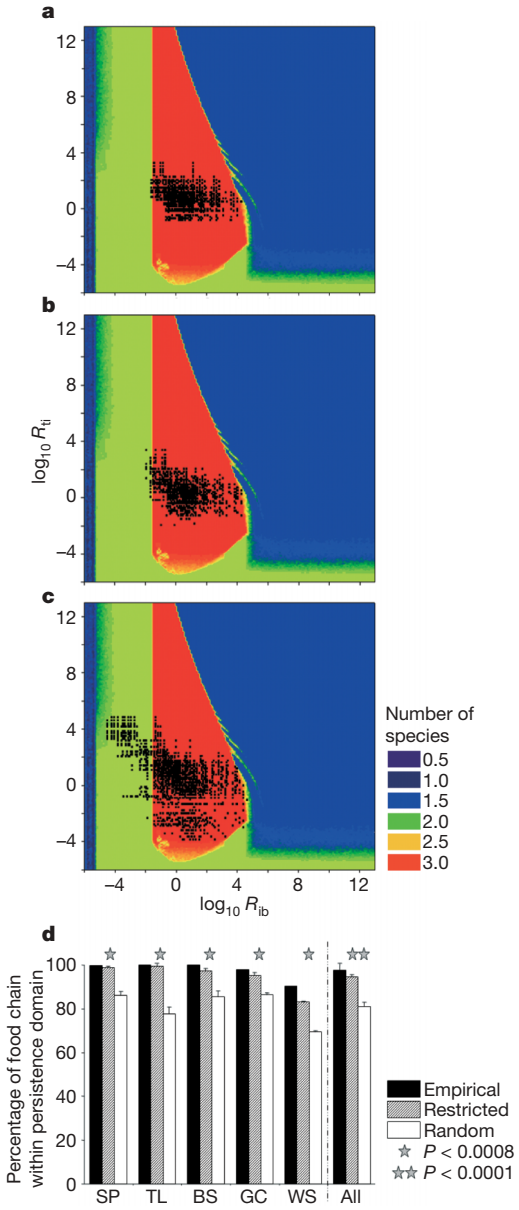

Figure 2 | Population persistence in tri-trophic food chains depending on R_{ti} and R_{ib}. **a–c**, Colours indicate the numbers of persistent species; red areas characterize a tri-trophic 'persistence domain'. Black points represent food chains of Skipwith pond under empirical food web structures (**a**), restricted rewiring (**b**) and random rewiring (**c**). **d**, Percentages of food chains within the persistence domain (SP, Skipwith pond; TL, Tuesday lake; BS, Broadstone stream; GC, Grand Cariçaie; WS, Weddell Sea) under empirical structures, restricted and random rewiring; results are shown as means and s.d. Stars indicate significant differences between the rewired versions of each food web.

distributions in these food webs strongly stabilize food-chain dynamics. To further explore this hypothesis, we randomly rewired the empirical food webs in a way that preserves the body masses of the species and the total number of links while completely disrupting the food-web topology ('random rewiring'; see Methods). An average of 81.0% ± 7.0% (mean ± s.d.) of these rewired food chains in each of the five food webs fell within the persistence domain (Fig. 2c, d, white bars). This probability is 4.1-fold the 19.6% probability of food chains with randomly distributed body masses within empirically observed ranges that are systematically and independently linked. However, 81% is significantly lower than the 97.5% probability that empirical food chains overlap with the persistence domain ($P < 0.01$). This difference suggests that, while the distribution of species' body masses found in natural food webs provides a substantial increase in the dynamical stability of possible food chains, topological properties of actual food chains might further facilitate food-web stability. To explore which topological properties can provide this additional stabilization, we tested whether correlations between the body mass and degree of species (that is, the number of predator and prey links of a population) drive this effect. To do this, we randomly rewired the food webs with a second randomization algorithm that preserves the body mass and degree of each species ('restricted rewiring'; see Methods). An average of 94.7% ± 6.2% (mean ± s.d.) of the food chains rewired in this restricted way lie within the persistence domain (Fig. 2b, d, grey bars). This probability is 4.8-fold the probability of food chains with randomly distributed body masses (19.6%) and differs significantly from randomly rewired networks (81.0%, $P < 0.05$), but it is not significantly lower than that in empirical food chains (97.5%, $P > 0.17$).

Overall, our results suggest that the distributions of and correlations between the body mass and degree of species within food webs are important mechanisms responsible for food-chain stability. Other topological properties of food webs seem to be of more minor importance. Instead, preserving allometric degree distributions realizes probabilities of tri-trophic stability similar to those found in empirical food webs. This conclusion seems qualitatively insensitive to variation in model parameters (see Supplementary Information). In the five natural food webs studied, the critically important mass–degree relationships are characterized by significant decreases in the number of predator links and significant increases in the number of prey links with increasing body masses of species (Table 1). These simple relationships were removed in the random procedure and retained in the restricted-rewiring procedure (Table 1). Our results seem to reveal a mechanistic basis of body-mass effects on population persistence in simple tri-trophic food chains. Scaling up our analyses to complex food webs suggests that population persistence there could be determined by similar constraints (see Supplementary Information). Although domains of stability using other functional responses also need to be explored, our results for the most widely used nonlinear functional response are of broad importance to ecology. Future extensions of our approach need to also address more variation between network models, species numbers and metabolic types of species to illuminate the generality of the results described here.

Community stability is known to be critically dependent on the body-mass distribution within food webs[3–5]. Here we explore potential mechanisms behind these stability effects by simulating tri-trophic food chains whose persistence is possible under a limited combination of species' body masses that describe a persistence domain. These mechanisms include energy limitation of the top species when predators are much smaller than their prey, and unstable enrichment-driven dynamics of intermediate species when they are much larger. Tri-trophic food chains are frequently parts of more complex motifs within food webs[9,10] that may exhibit more stable dynamics[13,19] or gain additional stability if large top predators couple either spatially separated food chains or other fast and slow energy channels[20–22]. Although ignoring such additional model complexity, the persistence domain predicted by our food-chain model is matched surprisingly well by 97.5% empirical food chains across five natural food webs. Further work on more complex food-web motifs is needed to obtain a better understanding of how body-mass-dependent population persistence scales up with system size from food chains to food webs.

Body masses impose physical constraints on who can hunt, handle and ingest whom in a community[23,24], which determines the diet breadth and foraging behaviour of individual species and topological food-web parameters[4,25,26]. To these relationships between body size and food webs, our study adds allometric degree distributions in which larger species feed on more prey and are consumed by fewer predators than small species. Our study provides a possible explanation for how these distributions may affect characteristics such as population persistence and food-web stability in natural communities. This connection between community-level degree distributions[27,28] and population biology suggests a fundamental bridge between food-web structure[8,28,29] and food-web dynamics[4,5]. Our results illuminate an allometric mechanism that may help to maintain the critically important biodiversity of natural ecosystems.

Table 1 | Allometric degree distributions: dependence of species' link structures (y) on body mass (x)

Food web	Topology	y	Regression equation	R^2	n	P
Skipwith pond	Empirical	No. of predators	$y = -1.00\log x + 5.91$	0.21	33	0.007
		No. of prey	$y = 2.47\log x + 21.01$	0.26	33	0.003
	Random	No. of predators	$y = -0.26\log x + 9.13$	0.05	33	0.20
		No. of prey	$y = -0.08\log x + 9.94$	0.004	33	0.71
Tuesday lake, 1984	Empirical	No. of predators	$y = -0.19\log x + 1.57$	0.47	25	0.0002
		No. of prey	$y = 0.71\log x + 12.61$	0.35	25	0.0017
	Random	No. of predators	$y = -0.03\log x + 3.50$	0.01	25	0.58
		No. of prey	$y = 0.03\log x + 4.30$	0.007	25	0.69
Broadstone stream	Empirical	No. of predators	$y = -0.80\log x - 1.91$	0.40	29	0.0003
		No. of prey	$y = 1.44\log x + 17.76$	0.15	29	0.04
	Random	No. of predators	$y = 0.31\log x + 7.85$	0.10	29	0.10
		No. of prey	$y = -0.24\log x + 3.02$	0.10	29	0.10
Grand Cariçaie, ClControl2	Empirical	No. of predators	$y = -0.54\log x + 4.39$	0.13	102	0.0002
		No. of prey	$y = 0.61\log x + 11.59$	0.05	102	0.03
	Random	No. of predators	$y = -0.06\log x + 7.36$	0.006	102	0.45
		No. of prey	$y = -0.05\log x + 7.44$	0.004	102	0.51
Weddell Sea shelf	Empirical	No. of predators	$y = -0.44\log x + 16.93$	0.02	275	0.03
		No. of prey	$y = 1.96\log x + 20.64$	0.10	275	<.0001
	Random	No. of predators	$y = 0.04\log x + 17.68$	0.002	275	0.50
		No. of prey	$y = 0.01\log x + 17.64$	0.0003	275	0.79

Linear least-square regressions of the number of predators and prey per species (y) on the $\log_{10}$ body masses (x) of the species of five food webs under empirical food-web structures and randomly rewired networks. Empirical networks and restricted rewired networks (not shown) show similar degree distributions, because the restricted rewiring algorithm preserves the number of predators prey per species; n is the number of invertebrate species in the food web.

METHODS SUMMARY

Simulations. A bioenergetic population dynamics model[6] defines the biomass evolution, dB/dt, of basal (b), intermediate (i) and top (t) species:

$$dB_b/dt = r_b G_b B_b - x_i y_i F_{ib} B_i/e \quad (1a)$$

$$dB_i/dt = -x_i B_i + x_i y_i F_{ib} B_i - x_t y_t F_{ti} B_t/e \quad (1b)$$

$$dB_t/dt = -x_t B_t + x_t y_t F_{ti} B_t \quad (1c)$$

where e is the assimilation efficiency, G_b is the logistic net growth (with carrying capacity K) and F is a type II functional response. Biological rates r, x and y (growth, metabolism and maximum consumption) scale with body mass, M: $r,x,y \propto M^{-0.25}$. r, x, y were normalized to the growth rate of basal species (thus, $r_b = 1$), and y was normalized to x. The maximum consumption rate was constant ($y = 8$); x increased with the body-mass ratio to basal species:

$$x_{i,t} = a\left(\frac{M_{i,t}}{M_b}\right)^{-0.25}$$

where a is a constant ($a = 0.2227$ when top, intermediate and basal species are invertebrates[16]). $R_{ti} = M_t/M_i$ and $R_{ib} = M_i/M_b$ are varied between 10^{-8} and 10^{13}, which influences their rates of metabolism (x) and consumption (xyF) per unit biomass. Initial biomass densities were random, simulations were run over 100,000 time steps. Maximum and minimum biomass densities of persistent populations ($B > 10^{-30}$) were recorded, and combinations of persistent R_{ti} and R_{ib} were defined as a 'persistence domain'. The averages of the top-down pressure per unit biomass on basal and intermediate species are $P_{b,i} = x_{i,t} y_{i,t} F_{ib,ti} B_{i,t}/B_{b,i}$, and the energy fluxes per unit biomass to intermediate and top species are $E_{i,t} = x_{i,t} y_{i,t} F_{ib,ti}$.

Rewiring. We compared R_{ti} and R_{ib} of the persistence domain with those of all tri-trophic food chains from five natural food webs (see Table 1)[7]. We created two additional versions of each empirical food web under random and restricted rewiring. For each treatment we calculated the fraction of food chains that were located within the persistence domain of our simulations under three conditions: empirical food web structures, restricted rewiring and random rewiring. Differences in results were evaluated by independent Mann–Whitney U-tests. Relationships between the degree and body mass of species were analysed by ordinary linear least-square regressions.

Full Methods and any associated references are available in the online version of the paper at www.nature.com/nature.

Received 13 July; accepted 12 October 2007.

1. De Ruiter, P. C., Wolters, V., Moore, J. C. & Winemiller, K. O. Food web ecology: Playing Jenga and beyond. *Science* **309,** 68–70 (2005).
2. Montoya, J. M., Pimm, S. L. & Solé, R. V. Ecological networks and their fragility. *Nature* **442,** 259–264 (2006).
3. Emmerson, M. C. & Raffaelli, D. Predator–prey body size, interaction strength and the stability of a real food web. *J. Anim. Ecol.* **73,** 399–409 (2004).
4. Loeuille, N. & Loreau, M. Evolutionary emergence of size-structured food webs. *Proc. Natl Acad. Sci. USA* **102,** 5761–5766 (2005).
5. Brose, U., Williams, R. J. & Martinez, N. D. Allometric scaling enhances stability in complex food webs. *Ecol. Lett.* **9,** 1228–1236 (2006).
6. Yodzis, P. & Innes, S. Body size and consumer–resource dynamics. *Am. Nat.* **139,** 1151–1175 (1992).
7. Brose, U. *et al.* Body sizes of consumers and their resources. *Ecology* **86,** 2545 (2005).
8. Williams, R. J. & Martinez, N. D. Simple rules yield complex food webs. *Nature* **404,** 180–183 (2000).
9. Bascompte, J. & Melian, C. J. Simple trophic modules for complex food webs. *Ecology* **86,** 2868–2873 (2005).
10. Milo, R. *et al.* Network motifs: Simple building blocks of complex networks. *Science* **298,** 824–827 (2002).
11. Hastings, A. & Powell, T. Chaos in a three-species food chain. *Ecology* **72,** 896–903 (1991).
12. Jonsson, T. & Ebenman, B. Effects of predator–prey body size ratios on the stability of food chains. *J. Theor. Biol.* **193,** 407–417 (1998).
13. McCann, K., Hastings, A. & Huxel, G. R. Weak trophic interactions and the balance of nature. *Nature* **395,** 794–798 (1998).
14. Muratori, S. & Rinaldi, S. Low- and high frequency oscillations in three-dimensional food chain systems. *SIAM J. Appl. Math.* **52,** 1688–1706 (1992).
15. Gard, T. C. Persistence in food webs: Holling type II food chains. *Math. Biosci.* **49,** 61–67 (1980).
16. Brown, J. H., Gillooly, J. F., Allen, A. P., Savage, V. M. & West, G. B. Toward a metabolic theory of ecology. *Ecology* **85,** 1771–1789 (2004).
17. Savage, V. M., Gillooly, J. F., Brown, J. H., West, G. B. & Charnov, E. L. Effects of body size and temperature on population growth. *Am. Nat.* **163,** E429–E441 (2004).
18. Rosenzweig, M. L. Paradox of enrichment: destabilization of exploitation of ecosystems in ecological time. *Science* **171,** 385–387 (1971).
19. Fussmann, G. F. & Heber, G. Food web complexity and chaotic population dynamics. *Ecol. Lett.* **5,** 394–401 (2002).
20. Koelle, K. & Vandermeer, J. Dispersal-induced desynchronization: from metapopulations to metacommunities. *Ecol. Lett.* **8,** 167–175 (2005).
21. McCann, K. S., Rasmussen, J. B. & Umbanhowar, J. The dynamics of spatially coupled food webs. *Ecol. Lett.* **8,** 513–523 (2005).
22. Rooney, N., McCann, K., Gellner, G. & Moore, J. C. Structural asymmetry and the stability of diverse food webs. *Nature* **442,** 265–269 (2006).
23. Woodward, G. *et al.* Body size in ecological networks. *Trends Ecol. Evol.* **20,** 402–409 (2005).
24. Brose, U. *et al.* Consumer–resource body-size relationships in natural food webs. *Ecology* **87,** 2411–2417 (2006).
25. Beckerman, A. P., Petchey, O. L. & Warren, P. H. Foraging biology predicts food web complexity. *Proc. Natl Acad. Sci. USA* **103,** 13745–13749 (2006).
26. Jonsson, T., Cohen, J. E. & Carpenter, S. R. Food webs, body size, and species abundance in ecological community description. *Adv. Ecol. Res* **36,** 1–84 (2005).
27. Montoya, J. M. & Solé, R. V. Topological properties of food webs: from real data to community assembly models. *Oikos* **102,** 614–622 (2003).
28. Stouffer, D. B., Camacho, J., Guimera, R., Ng, C. A. & Amaral, L. A. N. Quantitative patterns in the structure of model and empirical food webs. *Ecology* **86,** 1301–1311 (2005).
29. Cattin, M. F., Bersier, L. F., Banasek-Richter, C., Baltensperger, R. & Gabriel, J. P. Phylogenetic constraints and adaptation explain food-web structure. *Nature* **427,** 835–839 (2004).

Supplementary Information is linked to the online version of the paper at www.nature.com/nature.

Acknowledgements We thank U. Jacob for providing the Weddell Sea data; A. de Roos, E. Berlow, S. Scheu and M. Visser for comments; R. Williams for simulation programs; and N. Martinez for editorial assistance. Financial support was provided by the German Research Foundation.

Author Contributions S.B.O., B.C.R. and U.B. contributed equally to this work. All authors discussed the results and commented on the manuscript.

Author Information Reprints and permissions information is available at www.nature.com/reprints. Correspondence and requests for materials should be addressed to S.B.O. (sonotto@bio.tu-darmstadt.de).

METHODS

Model. Population dynamics of three invertebrate species in a food chain follows a bioenergetic model[6] of the biomass evolution (see equations (1)). $G_b = 1 - B_b/K$ and $F_{ib} = B_b/(B_0 + B_b)$; $F_{ti} = B_i/(B_0 + B_i)$ with a half saturation density B_0. Here, the fraction of the biomass removed from the resource population that is actually eaten is set to unity, which is often characterized as the mechanistically simplest model of predator–prey interactions[30]. The biological rates of production (W), metabolism (X) and maximum consumption (Y) follow negative-quarter power-law relationships with the species' body masses[16]:

$$W_b = a_r M_b^{-0.25} \quad (2a)$$

$$X_{i,t} = a_x M_{i,t}^{-0.25} \quad (2b)$$

$$Y_{i,t} = a_y M_{i,t}^{-0.25} \quad (2c)$$

where a_r, a_x and a_y are allometric constants[6]. The timescale of the system is defined by setting the mass-specific growth rate to unity (equation (3a)). Then the mass-specific metabolic rates of all species, x, are normalized by the timescale (equation (3b)), and the maximum consumption rates, y, are normalized by the metabolic rates:

$$r_i = 1 \quad (3a)$$

$$x_{i,t} = \frac{X_{i,t}}{W_b} = \frac{a_x}{a_r}\left(\frac{M_{i,t}}{M_b}\right)^{-0.25} \quad (3b)$$

$$y_{i,t} = \frac{Y_{i,t}}{X_{i,t}} = \frac{a_y}{a_x} \quad (3c)$$

Substituting equations (3a)–(3c) into equations (1a) and (1b) yields a population dynamic model with allometrically scaled and normalized parameters.

Here the body mass of the basal species, M_b, is set to unity, and the body masses of all other species, M_i and M_t, are expressed relative to the body mass of the basal species. This makes the results presented here independent of the body mass of the basal species.

Simulations. In simulations of tri-trophic food chains, the R values between the top and intermediate species (R_{ti}) and between the intermediate and basal species (R_{ib}) define the body masses M_i and M_t. We used constant values for the other model parameters: maximum ingestion rate $y_{i,t} = 8$ for invertebrate predators; assimilation efficiency $e = 0.85$ for carnivores; carrying capacity $K = 1$; half saturation density of the functional response $B_0 = 0.5$; allometric constant $a = a_x/a_r = 0.2227$ (top, intermediate and bottom species were simulated as invertebrates). We sought a mechanistic explanation for the influence of R on food-web stability by simulating food chains as the simplest multitrophic motif with energy transfer across several trophic levels. This characterizes complex natural food webs better than bitrophic consumer–resource relationships. Analyses of more complex motifs such as omnivory modules require knowledge about the relative interaction strengths of generalist predators with their multiple prey, which was not available for the natural food webs studied.

We varied R between the top and intermediate species ($R_{ti} = M_t/M_i$) and between the intermediate and basal species ($R_{ib} = M_i/M_b$) between 10^{-8} and 10^{13}, which decreased their rates of metabolism (x) and consumption (xyF) per unit biomass. Simulations started with uniformly random biomass densities ($0.05 < B_{t,i,b}\,(T = 0) < 1$) and ran more than 100,000 time steps (T) or until the largest species attained two biomass minima. We recorded the maximum and minimum biomass densities in the second half of the time series of the persistent populations ($B > 10^{-30}$) and defined a 'persistence domain' of combinations of R_{ti} and R_{ib} that enabled persistence of the three populations. For every time series we calculated the averages of the top-down pressure per unit biomass on the basal species, $P_b = x_i y_i F_{ib} B_i/B_b$, and the energy flux per unit biomass to the intermediate species, $E_i = x_i y_i F_{ib}$. Similar calculations yield the averages of the top-down pressure per unit biomass on the intermediate species and the energy flux per unit biomass to the top species.

Evaluation and rewiring. Subsequently, we compared the R_{ti} and R_{ib} values of the persistence domain with those of all tri-trophic food chains across five natural food webs: one from a stream (Broadstone stream), one from a pond (Skipwith pond), one from a lake (Tuesday lake, 1984), one terrestrial (Grand-Cariçaie, ClControl2) and one marine (Weddell Sea shelf) from a global data base[7]. To allow comparisons with our simulations, we studied only food chains of three invertebrate species that composed the vast majority of food chains in the empirical food webs, whereas few food chains include vertebrates or plant species. To test our hypotheses we created two additional versions of each of these empirical food webs under random and restricted rewiring. The 'random rewiring' algorithm conserved only the species' body masses and the total number of links, n, of the empirical food webs and randomly relinked n species pairs without any restrictions. The 'restricted rewiring' algorithm (see ref. 10 and references therein) randomly selects two predator–prey pairs and reconnects the predator of the first pair with the prey of the second pair and vice versa. This rewiring required that none of the new links already existed and ensured the conservation of the total number of predators and prey of each species along with their body masses and the total number of links in the network. We relinked n pairs of links in each food web 20 times to create a random rewired version of the network. Each of the two algorithms was applied to each of the five food webs studied with eight replicates. For each replicate we calculated the fraction of invertebrate food chains with body-mass ratios that were located within the persistence domain of our simulations under three conditions: empirical food web structures, restricted rewiring and random rewiring.

Statistics. Differences in these fractions between the three versions of the food webs were statistically evaluated by eight independent Mann–Whitney U-tests. In each test the five empirical probabilities were tested against five probabilities for each rewiring algorithm (randomly drawn from the eight replicates for each food web). Subsequently, each test was characterized by the highest of the eight P values. The relationships between the numbers of predator links and prey links and the body masses of the species were analysed by ordinary linear least-square regressions. Regressions were performed for each empirical replicate and one randomly rewired replicate of each of the five food webs.

30. Jeschke, J. M., Kopp, M. & Tollrian, R. Predator functional responses: Discriminating between handling and digesting prey. *Ecol. Monogr.* **72,** 95–112 (2002).